EFFECT OF CONTACT ANGLE ON EQUILIBRIUM SATURATION DURING MIST FILTRATION IN NONWOVEN AND FOAM MEDIA

S. Abishek[1,2,*], B.J. Mullins[1,2], A.J.C.King[2,3], G. Kasper[4], W. Heikamp[5]
[1] Occupation and Environment, School of Public Health, Curtin University, Australia
[2] Fluid Dynamics Research Group, Curtin Institute of Computing, Curtin University, Australia
[3] Department of Mechanical Engineering, Curtin University, Australia
[4] Institute for Mechanical Process Engineering and Mechanics, Karlsruhe Institute of Technology, Germany
[5] Raschig GmbH, Germany

ABSTRACT

Coalescence filtration using knitted, foam or nonwoven fibrous media is the widely applied in the industry for separation and recovery of liquid mists that are generated in many processes, including lubricated machining, compressors and engine crankcases. The dynamics of multi-component/ phase fluid transport and its interaction with the filter surface at the pore-scale and the contact angle dynamics are expected to significantly influence performance and efficiency of filtration processes. Most mist filters currently used in the industry are hydro- or oleophillic in nature, even though it is expected that philic filters will develop higher steady state saturation levels compared to phobic media. For hydro- or oleo-phobic media, it can be expected that once steady operation is reached, the total level of saturation in the filter media will be significantly lower, thus providing advantages in lower pressure drops and better overall performance. However, phobic media may possibly result in greater levels of aerosol re-entrainment and a greater potential for clogging by (other) solid particles since parts of the filter may not be fully wetted. Yet, the literature on the influence of contact angles and its dynamics on mist filtration characteristics and transport of collected fluid in the filter (including drainage and re-entrainment) is sparse. Practical difficulties in the measurement of contact angles on micro-/nano-fibres have also been a consistent dilatory factor in accurate quantification of the wetting characteristics of filter media. Computational fluid dynamics (CFD) simulations at the pore-scale with interface capturing techniques offer a unique advantage in enabling parameters such as contact angles and other fluid properties to be precisely defined - and hence ideal for parametric characterization of the filter performance. With the aim of isolating the influence of contact angles on the transport of collected liquid in a filter medium, in the present study, CFD simulations are carried out where the filter is pre-saturated with Diethylhexyl Sebacate (DEHS) which is flushed with air (at constant flow rate). Two structurally different types filter media, nonwoven and foam, with similar properties such as fibre (or element of foam) diameter, packing density and size are used for the present study to compare the influence of contact angles across types of filters. The present simulations reveal that there can be a specific contact angle (between 60° and 120°) for both the types of filters (and operating conditions) considered where the saturation in the medium can drop close to zero resulting in a possibly self-cleaning mist filter.

KEYWORDS

Aerosol, Mist filtration, Foam, Fibre, CFD, VOF

1 INTRODUCTION

Efficient separation of liquid aerosols or mists is of significant importance in many process and automotive applications. Liquid aerosols are typically generated by industrial compressors, lubricated machining and cutting processes and in engine crankcases. One of the most effective and commonly used methods to treat oil-mist is through the use of highly porous filters of different types including nonwoven fibrous, foam or knitted media [1, 2, 3].

Most industrial oil-mist filters are oleophillic, with relatively well described, though difficult to accurately model, behaviour [4, 5, 6]. Such filters will rapidly become clogged with oil, causing an increase in pressure drop and (usually) a decrease in efficiency, until they attain a state of equilibrium. This process has been described in the literature [7, 8, 9, 10, 11], with several studies describing the process by which a clean filter reaches the equilibrium state. Although some of the mist filters used in industry have been constructed of oleophobic fibres, or a combination of phillic and phobic media, phobic filters have not yet received significant attention in the literature.

It is expected that oleophobic filters may reduce saturation due to lower surface energy on the filter surface which would result in the coalesced oil not fully wetting the filter media. However, given the lower surface energy, re-entrainment from the oleo-phillic filters may be more pronounced [12]. The state of being (oleo)phobic or (hydro)phobic, with respect to fibres is generally defined by the presence of clamshell droplets with a contact angle between $\sim 60^\circ$ and 180° - the latter generally being regarded as “super”-()phobic. However, the few filter studies which have examined phillic or phobic media generally only define the media in this category, rather than giving a specific contact angle.

A review of the literature suggests that there have been relatively few studies that have examined the performance of oleophobic fibres and/ or filter media [11, 12, 13, 14, 15, 16]. Most of the studies have also focused on the isolated effects of aerosol or droplets (mists) on single phobic fibres [11, 15], the capillarity of phobic media [13], or filter surface energy measurements [11]. However, it is noted that the performance of phobic media as mist filters has received little attention [12, 16].

Experimental determination of contact angles on filter media is exceedingly difficult due to limitations imposed by the resolutions of current imaging equipment. Even precise contact angle measurements of a droplet on a single fibre is not elementary, as measurements can typically only be performed at 2-4 discrete points on a curved surface. Contact angles can be measured on the surface of phobic media, however the relationship to single fibre measurements are not fully validated.

Pore-scale computational fluid dynamics (CFD) simulations of the mist filtration process using advanced droplet- and interface-tracking approaches provide unique advantages in allowing precise definition of contact angles, and other interfacial and fluid properties [17]. However, the significant computing power required for resolving the flow physics at pore-scales and the difficulty in representing a suitable filter structure (often reconstructed from scans of real media) can be a challenging task. In a separate study [18, 19], the authors have demonstrated a methodology for generating virtual media that qualitatively and quantitatively reflects real filters and CFD-suitable computational mesh for two types of mist filter media (foam and nonwoven fibrous). The process of mist filtration at steady state can be characterized by relatively large levels of fluid saturation, dynamic fluid redistribution, re-entrainment, drainage, etc. To

isolate the effects on contact angle on the transport of collected liquid alone in the filter media during the process of mist filtration, in the present study, computational simulations are carried out where the filter is pre-saturated with Diethylhexyl Sebacate (DEHS) which is flushed with air (at constant flow rate). Two structurally different types filter media, nonwoven and foam, with similar properties such as fibre (or element of foam) diameter, packing density and size are used for the present study to additionally compare the influence of contact angles across types of filter media.

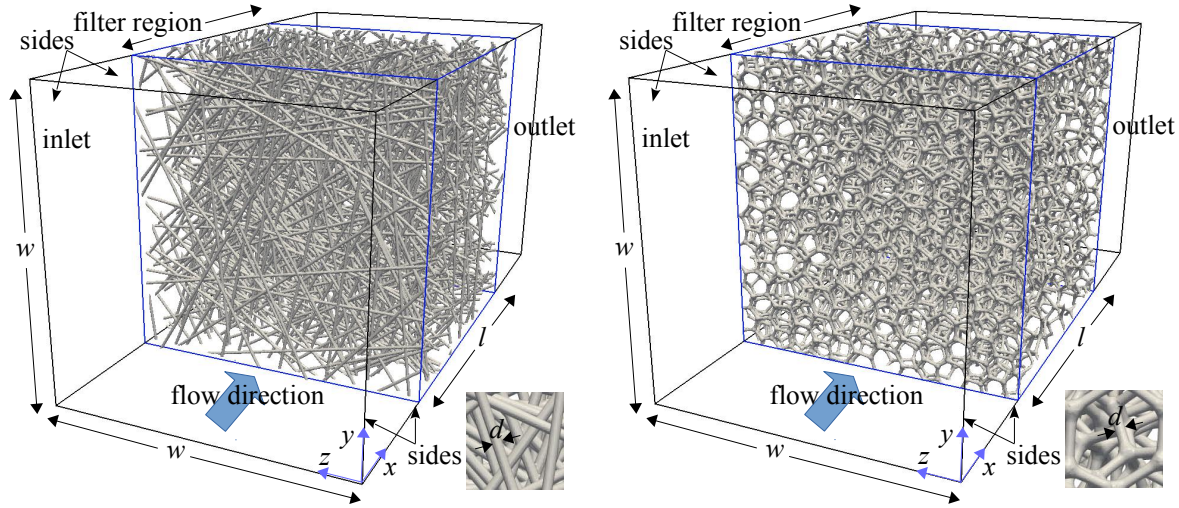

(a) schematic for nonwoven media (b) schematic for foam media

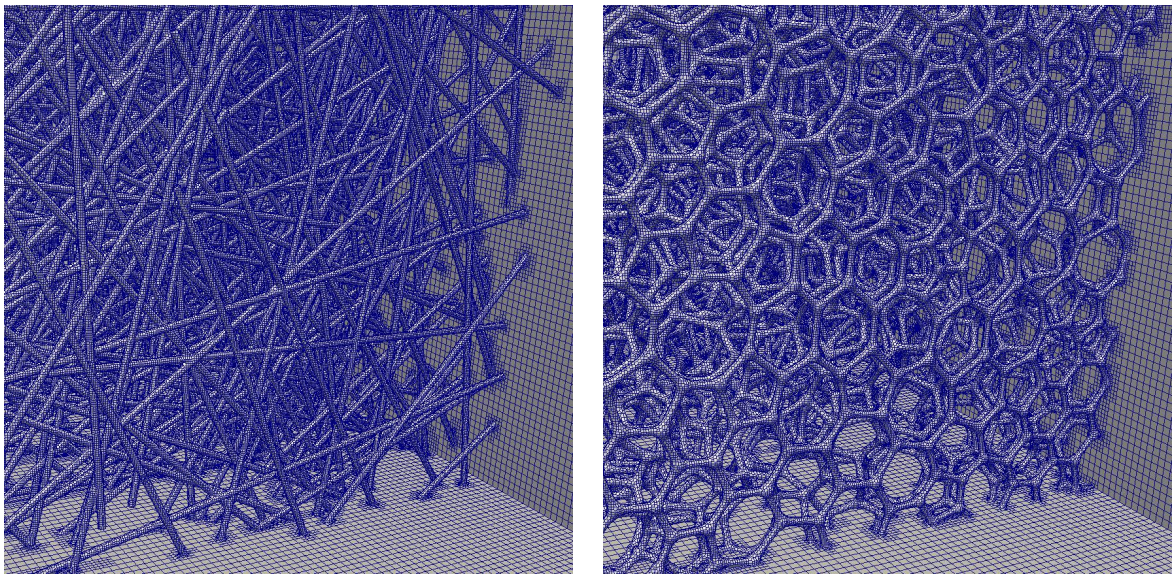

(a) mesh for nonwoven media (b) mesh for foam media

Figure 1: Schematic of the computational domains and representative structure of the nonwoven and foam media used in the present study

2 COMPUTATIONAL METHODOLOGY

The filter media employed for the simulations are generated using a novel in-house technique. The details of the methodology and work flow for the generation of the filter geometries and CFD suitable computational mesh is elaborated in [18, 19], and

hence omitted here for brevity. The schematic of the computational domains used for the present simulations are illustrated in Fig. 1, where representative sections of the nonwoven and foam media are shown in Figs. 1(a) and Fig. 1(b) respectively. Representative sections of the corresponding computational mesh employed for the two media are illustrated in Figs. 1(c) and Fig. 1(d) respectively. Two types of simulations are carried out - (i) with air alone through dry filter media, and (ii) air flow with filter medium pre-saturated with DEHS oil. For the latter,the section of the computational domain indicated as 'filter region' in the figure (blue-box) is initially ($t = 0$) filled with DEHS to represent a 'dipped filter', while the rest of the domain is filled by air. A constant flow of air is imposed at the 'inlet' of the domain for all times $t > 0$ until steady state is reached - which is ascertained by monitoring the transience of: (i) pressure drop ($\triangle p_{\text{air-oil}}$), (ii) oil saturation in the filter region (α_{oil}), (iii) location of the centre of mass of oil in the filter region (x_{com}) and equivalent thickness of oil at the downstream face of the filter (λ_{eq}) calculated as $(V_{\text{oil}} - V_{\text{oil, filter}})/w^2$ where, w is the width of the filter cross-section (and computational domain). The fibre (and element of foam) diameter, length of the fibre along the direction of mean flow, and size of the geometries are considered constant as $d = 20$ μm, $l = 0.002$ m and $w = 100 \times d$, respectively. The mean air flow velocity applied at the inlet for both, the single phase as well as the multiphase experiments, is fixed at $u_{\text{o}} = 0.6$ m/s, corresponding to a Reynolds number Re$= \rho_{\text{air}} u_{\text{o}} d/\mu_{\text{air}} = 0.8$ and a capillary number $Ca = \mu_{\text{air}} u_{\text{o}}/\sigma = 3.375 \times 10^{-4}$. The effect of contact angle (θ_{e}, between DEHS oil and the filter surfaces) is investigated in the range 20°-170°, encapsulating most oleophillic and and oleophobic media used in the industry.

To enable comparison of the effect of contact angle between the two types of filter media, it was ensured that the filter packing density remained nearly equal between the two media. They are calculated to be α_{s}=0.035 for the nonwoven filter and 0.039 for the foam media. The total mesh size, determined based on a mesh and domain sensitivity study for the nonwoven and foam media are 6.5$\times 10^6$ and 4.7$\times 10^6$ cells, respectively. The single phase pressure was found to be mesh and domain-size independent to within $< 5\%$ while the two-phase pressure drop, liquid saturation at steady state, centre of mass of the liquid retained in the filter region, and the equivalent thickness of the liquid at the downstream face of the filter were found to be mesh and domain-size independent to within $\approx 10\%$. The larger variation in the two-phase quantities are attributed to the greater sensitivity of the two-phase flow to the inherently irregular structure of the filter media at the pore-scales.

The governing conservation equations of mass (continuity) and momentum for the single phase simulations are solved at steady state using the finite volume based computational solver $simpleFOAM$, available within the open-source CFD framework OpenFOAM. The second series of simulations involving both air and DEHS are carried out using the transient $interFOAM$ solver which uses an algebraic volume-of-fluid (VOF) approach [20] for tracking the air-oil interface. Sufficient interface compression was used (> 1) for the simulations based on the mesh resolution for each case for accurate representation of the local interface curvature with minimal numerical smearing. The general set of governing equations are available in [20, 21] and hence omitted here for brevity. To ensure no spatial anomalies (at the pore-scale) exist in the virtual media, which may adversely influence the simulations, a check is carried out to evaluate the local packing density distribution in the largest domains of the foam and nonwoven media. The local packing density distribution, evaluated by averaging the solid volume

fraction in the direction parallel to mean flow along segmented locations in a plane perpendicular to the mean flow, for the geometries considered for the present simulations are included in [19].

All computational simulations reported in this paper were carried out using 48-240 cores on the supercomputing facility Magnus with a Cray XC40 system at Pawsey Supercomputing Centre, Perth, Australia.

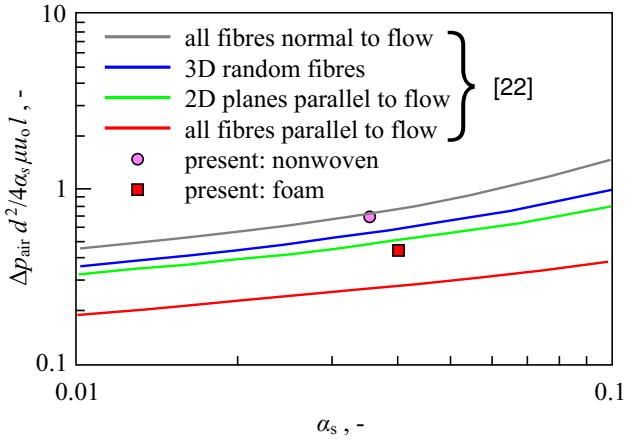

Figure 2: Comparison of dimensionless pressure drop predicted from the present simulations against theoretical predictions by Spielman and Goren [22]

3 RESULTS AND DISCUSSION

To validate the characteristics of the virtual filter media generated by the present methodology, single phase simulations using air were conducted at a prescribed velocity of $u_o = 0.6$ m/s through the nonwoven and foam media. The pressure drops obtained from the present simulations (represented in dimensionless form) are shown in Fig. 2 for the two types of media. The values from the theoretical model of Spielman and Goren [22] for four types of filters where: (i) all fibres are normal to flow, (ii) 3D random fibres, (iii) all fibres are in 2D plans parallel to flow and (iv) all fibres are parallel to flow, are shown for comparison. It is seen from the figure that the predicted pressure drops for both the types of media are in good agreement with the literature.

The effect of contact angle on the two phase flow through the two filter media is carried out in the range 20°-170°. Snapshots of the (near) steady state oil saturation profile inside the filters is illustrated in Fig. 3 for three contact angles 20°, 60° and 120°. For each contact angle and filter media shown in the figure, the 2D (orthogonal) views of the saturation from the inlet (flow: into the plane of the paper) and side views () flow: left to right) are shown below the 3D perspective (flow: out of the plane of the paper) representations. It can be seen from the figures that for both, nonwoven and foam media, the liquid saturation in the filter region decreases, as expected, with an increase in contact angle. It can be seen from the figures that for relatively lower contact angles, larger contiguous liquid structures exist in the filter region at steady state. With the further inflow of liquid mist (not included in the present study), this would typically result in clogging of the filter media leading to relatively greater pressure drops. Due to lower energy/ adhesion of the oil to the surface of the filters at higher contact angles, it can be seen from the figures that the independent or segregated liquid structures prefer a more spherical form (the size of which may be controlled by the local pore-size distribution). Through visual observation of processed videos of the

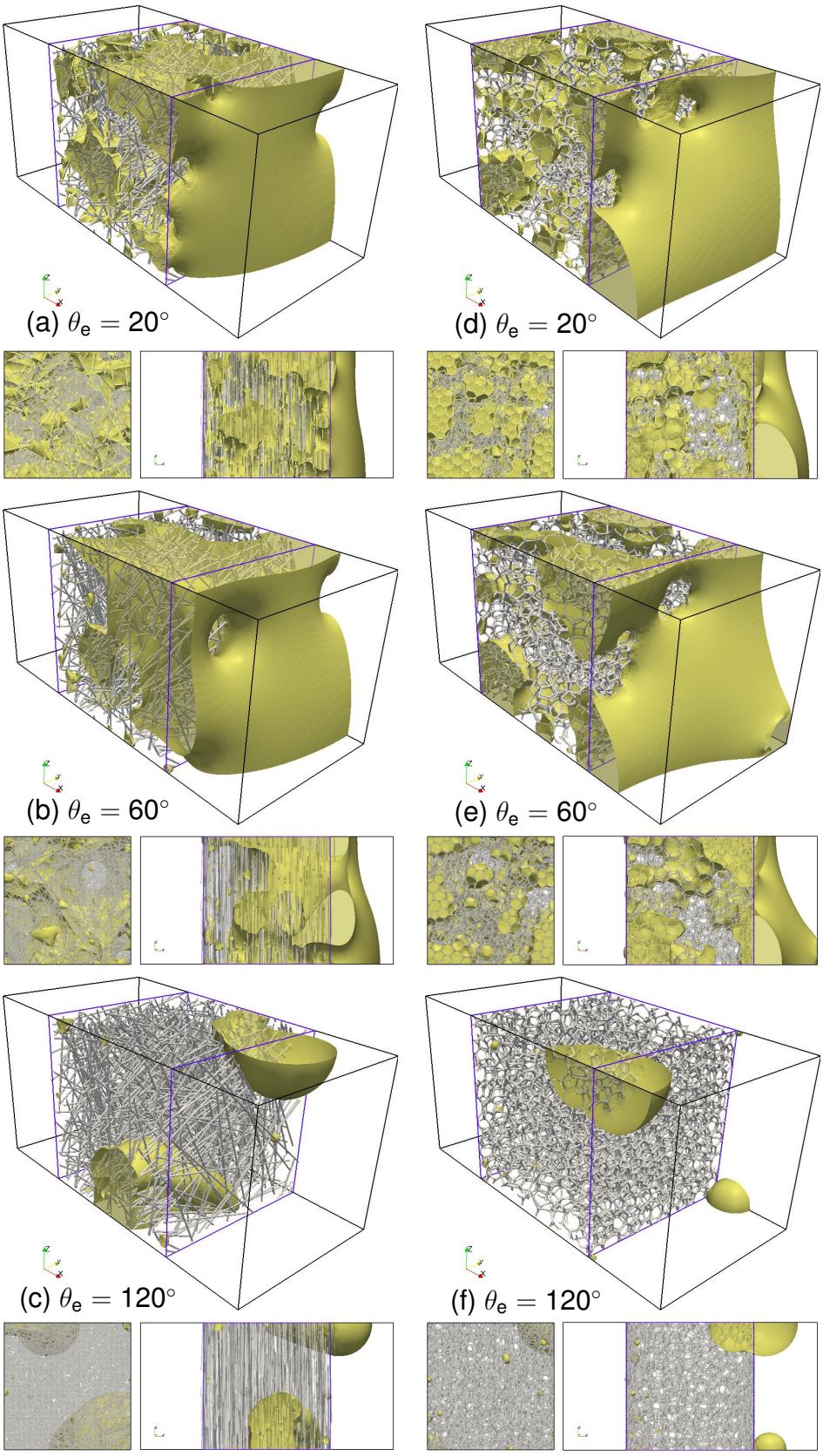

Figure 3: Comparison of the (near) steady state fluid saturation in the nonwoven and foam media for different contact angles

entire process as well as from Figs.3(c,d) it can be seen that an increase in contact angle results in larger liquid parcels to be ejected from the domain. It is also seen

from the figures that an increase in contact angle results in an increase in the size of the air channels in the liquid film at the downstream face of the filter, through which air escapes - to the extent that no liquid remains for the case θ =120° shown. This implies the existence of a critical point for the relationship between capillary and air-flow forces - with important implications for drainage and re-entrainment in mist filtration processes. The aforementioned observations are found to be true for both the types of filter media considered in the present research.

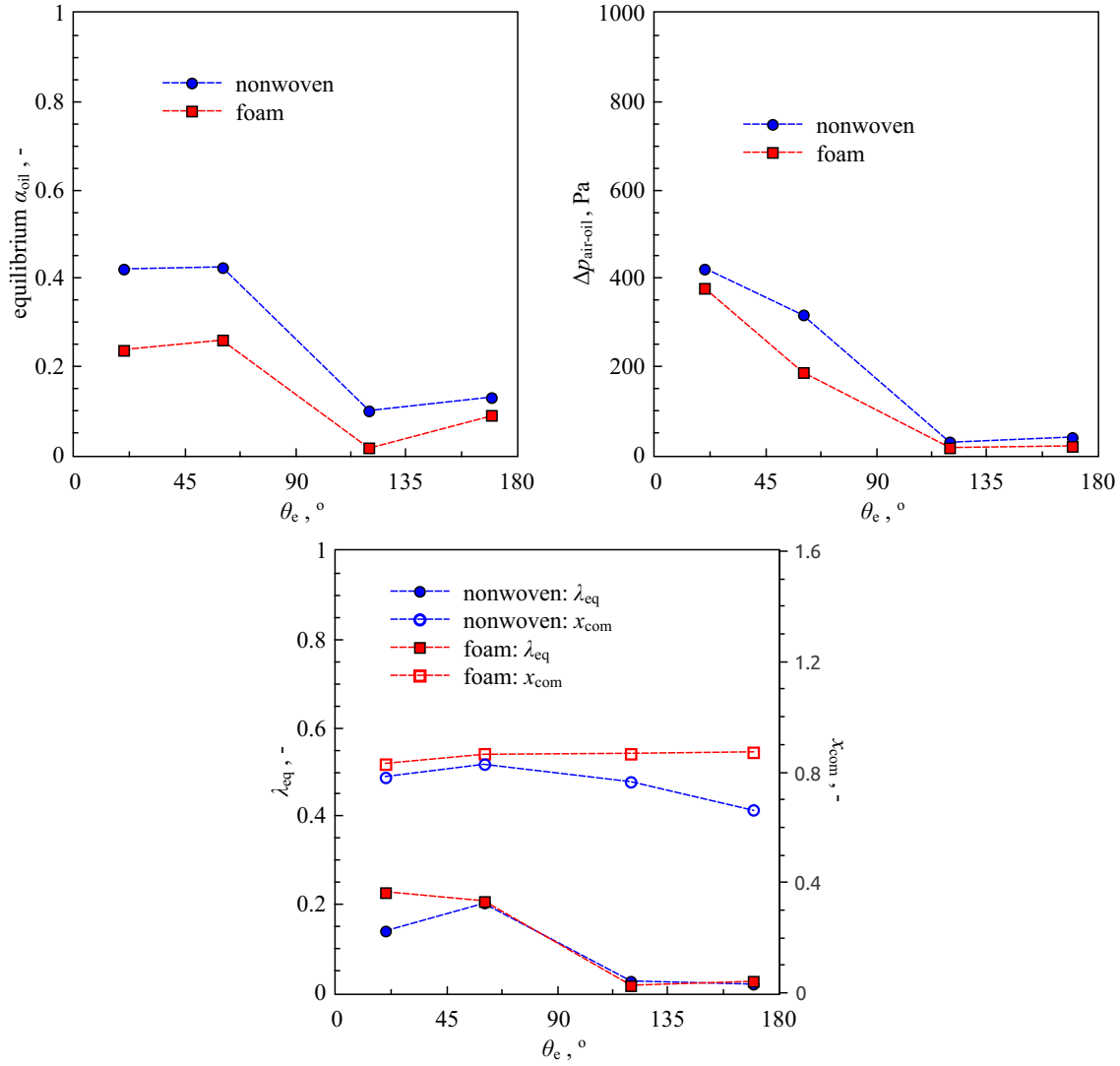

Figure 4: Comparison of the effect of contact angle on the steady state saturation, pressure drop, location of the centre of mass of retailed oil and the equivalent thickness of oil at the downstream face of the filter between nonwoven and foam media

The steady state values of the oil saturation inside the filter region, two-phase pressure drop, location of the centre of mass of retailed oil and the equivalent thickness of oil at the downstream face of the filter for nonwoven and foam media are presented in Fig. 4. In agreement with the qualitative observations outlined in the preceding discussion on Fig. 3, it can be seen that an increase in contact angle results in a commensurate reduction in the oil saturation at steady state. The slight increase in the oil saturation in the filter from $\theta = 120°$ to $\theta = 180°$ can be attributed to the small

amount of liquid that is retained - possibly a numerical anomaly, the effects of which may reduce for any larger domain considered for the simulations. It is pointed out that the domain size chosen for the study was based on series of systematic tests carried out with successively larger domains, but for a contact angle of $\theta = 20^\circ$ [19]. To abate any such (albeit minor) artifacts of the computational simulations and for increased accuracy of the predictions, it is necessary to carry out similar domain studies for each contact angle considered. As a direct consequence of the reduction in fluid saturation inside the filter, the two phase pressure drop is seen to decrease to a value nearly equal to the single phase pressure drops for the two filters expected. This is indicative that there may be an optimum value of contact angle that may potentially aid in drainage and/ or aid in self-cleaning of the filter at run-time benefiting mist filtration using such oleo-phobic filter with greater efficiency per pressure loss. It is interesting to note that while the saturation in the filter domains, for both filters vary only marginally between contact angles $\theta = 20^\circ$ and $\theta = 60^\circ$, while there is comparatively larger change in the two-phase pressure drop. This can be attributed to the relatively greater liquid film thickness at the downstream face of the filter (as well as greater volume of the liquid downstream from the entrance of the filter) that results in greater resistance to air-flow.

4 CONCLUSIONS

Mist filtration processes are regarded to be highly influenced by the dynamics of wetting at the pore-scales. Yet, the current understanding of the influence of oleo- hydrophobicity or -philicity on the characteristics of mist filtration is sparse, particularly due to several practical difficulties and limitations in accurate measurement of liquid and characterization of contact angles and contact line dynamics on micro or nano filter media. Computational fluid dynamics analysis using highly resolved interface tracking approaches provide a unique opportunity to carry out parametric analysis of such pore-scale processes due to the ease in precisely defining the contact angles and other fluid or interface properties. In the present research, CFD simulations using the VOF technique are carried out to study the influence of oil-filter contact angles on the dynamics of two-phase (DEHS-air) flow through two types of filter media - nonwoven and foam. With the intent of isolating the influence of contact angle on the transport of the of the retained oil (characteristic of steady state filtration), the present simulations consider pre-saturated filter media from which oil is flushed out using a constant flow of air until steady state (or steady saturation) is reached. It is seen from the simulations that while all other fluid properties and flow conditions are kept constant, a change in oil-filter contact angle alone has a tremendous influence on the two-phase fluid dynamics. The simulations reveal that there could be a threshold contact angle for a given fluid-pair or flow rate, when the saturation in media can reduce to near-zero, implying that the filter may be able to drain at run-time under real conditions - with minimal pressure drop. However, further research on larger geometries and other parametric conditions, as a direct extension of the present study is required to validate this observation and identification of a threshold contact angle for optimum filter performance, if any.

5 ACKNOWLEDGEMENTS

The authors acknowledge the support of Australian Research Council under Linkage Grant (LP140100919) and Raschig GmbH, Germany for carrying out this research. This work was also supported by the Pawsey Supercomputing Centre, Perth, Western Australia with funding from the Australian Government and the Government of Western Australia, through the use of its advanced computing facility and resources.

References

[1] R. Mead-Hunter, A. J. C. King, B. J. Mullins, Aerosol-mist coalescing filters - a review, Separation and Purification Technology 133 (2014) 484–506.

[2] B. J. Mullins, A. J. C. King, R. D. Braddock, Modelling the influence of filter structure on efficiency and pressure drop in knitted filters, Proceedings of the 19th International Congress on Modelling and Simulation, MODSIM2011, Perth, Australia (2011) 579–585.

[3] M. Khosravi, S. Azizian, Synthesis of a novel highly oleophilic and highly hydrophobic sponge for rapid oil spill cleanup, ACS Applied Materials and Interfaces 7 (2015) 25326–25333.

[4] P. C. Raynor, D. Leith, The influence of accumulated liquid on fibrous filter performance, Journal of Aerosol Science 31 (2000) 19–34.

[5] R. M.-H. R, R. D. Braddock, D. K. D, N. Merkel, G. Kasper, B. J. Mullins, The relationship between pressure drop and liquid saturation in oil-mist filters - predicting filter saturation using a capillary based model, Separation and Purification Technology 104 (2013) 121–129.

[6] T. Frising, D. Thomas, D. Bemer, P. Contal, Clogging of fibrous filters by liquid aerosol particles: experimental and phenomenological modelling study, Chemical Engineering Science 60 (2005) 2751–2762.

[7] A. Charvet, Y. Gonthier, E. Gonze, A. Bernis, Experimental and modelled efficiencies during the filtration of a liquid aerosol with a fibrous media, Chemical Engineering Science 65 (2010) 1875–1886.

[8] P. Contal, J. Simao, D. Thomas, T. Frising, S. Calle, J. C. Appert-Collin, D. Bemer, Clogging of fibre filters by submicron droplets. phenomena and influence of operating conditions, Journal of Aerosol Science 35 (2004) 263–278.

[9] A. B. A, B. J. Mullins, Influence of flow-interruption on filter performance during the filtration of liquid aerosols by fibrous filters, Separation and Purification Technology 90 (2012) 53–63.

[10] A. Bredin, R. A. O'Leary, B. J. Mullins, Filtration of soot-in-oil aerosols: why do field and laboratory experiments differ, Separation and Purification Technology 96 (2012) 107–116.

[11] R. Mead-Hunter, T. Bergen, T. Becker, R. A. O'Leary, G. Kasper, B. J. Mullins, Sliding/ rolling phobic droplets along a fiber: measurement of interfacial forces, Langmuir 28 (2012) 3483–3488.

[12] B. J. Mullins, R. Mead-Hunter, R. N. Pitta, G. Kasper, W. Heikamp, Comparative performance of philic and phobic oil-mist filters, AIChE 60 (8) (2014) 2976–2984.

[13] B. J. Mullins, R. D. Braddock, Capillary rise in porous, fibrous media during liquid immersion, International Journal of Heat and Mass Transfer 55 (2012) 6222–6230.

[14] S. B. K. Y. M. J. B H Park, M H Lee, Evaluation of the surface properties of ptfe foam coating filter media using xps and contact angle measurements, Surface Science 257 (2012) 3709–3716.

[15] B. J. Mullins, R. D. Braddock, I. E. Agranovski, R. A. C. R. A. O'Leary, Observation and modelling of clamshell droplets on vertical fibres subjected to gravitational and drag forces, Journal of Colloidal Science 284 (2005) 245–254.

[16] B. J. Mullins, R. D. Braddock, I. E. Agranovski, Particle capture processes and evaporation on microscopic scale in wet filters, Journal of Colloid and Interface Science 279 (2004) 213–227.

[17] R. Mead-Hunter, A. J. C. King, G. Kasper, B. J. Mullins, Computational fluid dynamics (CFD) simulation of liquid aerosol coalescing filters, Journal of Aerosol Science 61 (2013) 36–49.

[18] S. Abishek, B. J. Mullins, A. J. C. King, G. Kasper, W. Heikamp, Generation of realistic nonwoven and foam filter media and mesh for filtration simulations using open-source tools, FILTECH-2016, International Conference and Exhibition for Filtration and Separation Technology, Cologne, Germany (2016) –.

[19] S. Abishek, B. J. Mullins, A. J. C. King, G. Kasper, W. Heikamp, Influence of filter domain size on the simulations of gas-liquid filtration in nonwoven and foam media, FILTECH-2016, International Conference and Exhibition for Filtration and Separation Technology, Cologne, Germany (2016) –.

[20] S. S. Deshpande, L. Anumolu, M. F. Trujillo, Evaluating the performance of the two-phase flow solver interfoam, Computational Science and Discovery 5 (2012) 014016–1–36.

[21] S. Abishek, A. J. C. King, R. Narayanaswamy, Dynamics of a taylor bubble in steady and pulsatile co-current flow of newtonian and shear-thinning liquids in a vertical tube, International Journal of Multiphase Flow 74 (2015) 148–164.

[22] L. Spielman, S. L. Goren, Model for predicting pressure drop and filtration efficiency in fibrous media, Current Research 2 (4) (1968) 279–287.